

Implicit Boundary Modeling (*BOUNDSIM*)

Jason A. McLennan and Clayton V. Deutsch

Centre for Computational Geostatistics
Department of Civil & Environmental Engineering
University of Alberta

Boundary modeling is a crucial part of natural resource characterization. Geostatistical estimation and simulation employ stationary random function models within volumetric boundaries to predict regionalized petrophysical properties of interest. Moreover, there is often significant global uncertainty in volumetric boundaries depending on the amount of sample and geological data available. There is a growing need for fast, objective, flexible, and geologically realistic boundary models accounting for global uncertainty. This paper presents and describes a novel boundary modeling algorithm with these features. Explicit or manually digitized volumetric boundaries are common, but do not capture volumetric uncertainty since these methods are time consuming, subjective, and non-repeatable. BOUNDSIM is an implicit boundary modeling methodology that automates the construction of fast, objective, and flexible probabilistic boundary surfaces built at any desired position of risk and resolution. Examples are presented to illustrate the methodology, practice, and results.

Background

Boundary modeling is an essential preliminary step for numerical mineral deposit and petroleum reservoir modeling. Geostatistical estimation and simulation of petrophysical properties is applied with stationary random functions within geometric limits imposed by volumetric bounding surfaces. Choosing the number of domains or volumes amounts to the most important aspect of a decision of stationarity. Boundary modeling has a significant impact on estimates of recoverable reserves, economic forecasting, and production planning.

Two general classes of boundary modeling methods are available, explicit and implicit. The traditional *explicit* method of boundary modeling implemented in nearly all general mining software packages relies heavily on manual digitization [1, 2]. These methods present some important practical limitations and challenges for modern resource characterization projects. Most importantly, explicit methods are incapable of assessing global uncertainty. Implicit methods, in contrast, are capable of automating production of multiple probabilistic boundaries collectively representing global uncertainty. *BOUNDSIM*, presented in this work, is an implicit approach.

The most important advantage of the implicit approach is access to global uncertainty, that is, structural or geological compartmentalization uncertainty. This type of uncertainty can have a significant influence on production uncertainty in various mining and petroleum settings. Figure 1 illustrates a schematic 2D example of an explicit boundary versus a set of implicit boundaries. The ore-waste boundaries are to be defined from four conditioning drillholes. A typical explicit ore-waste boundary is shown on the left. In practice, this would involve a subjective digitization procedure. Three implicit ore-waste boundaries are shown on the right. Using the implicit approach, constructing these boundaries is objective and fast. Most importantly, however, the small (B1), medium (B2), and large (B3) boundary models can be adopted according to

conservative, medium, or aggressive positions on global volumetric uncertainty. The green arrows show any position of risk is easily assumed by expanding or contracting the boundary. This access to uncertainty is not possible with the explicit approach.

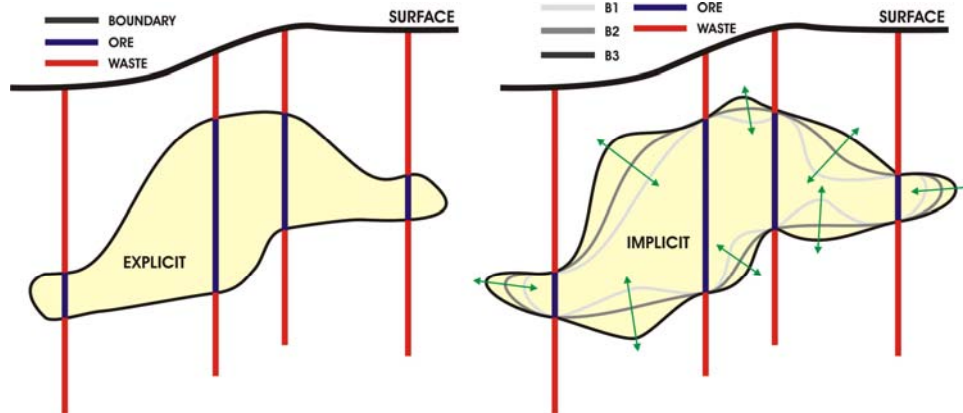


Figure 1: A small 2D schematic example illustrating an explicit boundary model (left) compared to a set of implicit boundary models (right). The implicit modeling method allows easy access to global volumetric uncertainty by expanding or contracting the boundary away from the four conditioning drillholes (green arrows).

The Decision of Stationarity

Conventional geostatistical estimation and simulation is applied with stationary random functions SRF's. The decision of stationarity is one of deciding the number of SRF's appropriate for modeling a single attribute. Separate decisions of stationarity are made for each attribute of interest. These decisions always balance the level of homogeneity with the number of available data within potentially separate domains. Consider the extremes. The most homogenous domain would surround a single sample datum; however, such a solitary sample is inadequate to reliably parameterize the set of SRF models, one for each sample location. By pooling all possible sample data together, there may be an adequate database for reliable inference of the single SRF model, but then there also exists a significant risk of masking key heterogeneous or compartmentalized features that could have otherwise been modeled by more than one SRF. Each setting involves a unique balance of these two factors, the degree of homogeneity and amount of available data.

Decisions of stationarity are made in a staged fashion according to a flowchart like the one shown in Figure 2. Moving through the scale, decisions of stationarity increase in resolution as the boundary surfaces surrounding assumed homogeneous regions shrink. In the first stage, for example, geological homogeneity is assumed and a single SRF is adopted inside a bounding surface that approximates the global mineral or hydrocarbon accumulation limits (red line). The enclosed SRF first order expected value and second order covariance function are then inferred from the available sample data to predict at unsampled locations within these limits. Further down the scale in Figure 2, higher resolution decisions of stationarity associated with more than one boundary surface are considered when the decision of stationarity at the previous level on the flowchart is deemed inappropriate in that there are enough geological data and information to suggest and model more than one SRF. The next stage could involve defining a separate SRF model boundary surfaces enclosing net and non-net material (broken green line). And continuing to follow Figure 2 as an example, geological homogeneity can be assumed and SRF's can be

adopted inside boundaries outlining structural or systems tract boundaries (LST ~ low-stand systems tract; FSST ~ falling stage systems tract; HST ~ high-stand systems tract; TST ~ transgressive systems tract). These boundaries are shown with broken yellow lines. Finally, at the highest resolution, distinct rocktype or facies boundaries could be defined to separate the SRF models.

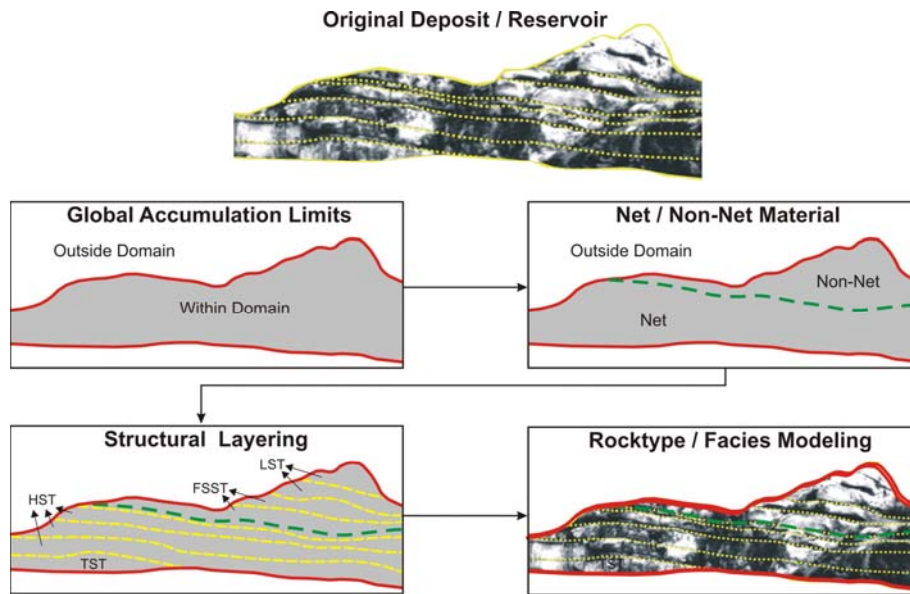


Figure 2: An illustration of the geometrically staged fashion in which decisions of stationarity are made. At each stage, different boundary surfaces are defined and modeled.

Explicit or implicit boundary modeling constructs the boundaries needed to separate different SRF models according to the prior decision of stationarity and position on a scale similar to what is shown in Figure 2.

Stochastic or probabilistic boundary modeling methods for rocktype and facies limits at the last stage of Figure 2 are already quite mature. There is a vast library of literature and implementation procedures for various cell-based methods such as sequential indicator simulation [3, 4, 5] and perhaps more geologically realistic object-based methods [3, 6, 7]. The algorithms and tools for stochastic structural surface modeling are becoming increasingly mature [8, 9, 10] and are a viable alternative to deterministic methods. However, there is little emphasis in the literature on probabilistic boundary modeling methods for the larger-scale types of boundaries referred to in the earlier stages of Figure 2. These types of boundaries are often drawn explicitly or deterministically with no direct account for global uncertainty. This work especially addresses the need for objective and probabilistic large-scale boundary surfaces.

Boundary Modeling Criteria

Before reviewing explicit boundary modeling in more detail, showing existing implicit methods, or presenting *BOUNDSIM*, six different criteria for viable boundary modeling algorithms are first defined:

1. *Simplicity*: The algorithm should be relatively straightforward to implement;

2. *Speed*: The algorithm should be capable of creating multiple boundary models in a reasonable amount of time;
3. *Subjectivity*: The algorithm should avoid personality and subjective interpretation in order to be repeatable;
4. *Flexibility*: The algorithm should be readily amenable to incorporate incremental geological data and information;
5. *Uncertainty*: The algorithm should allow for the access to boundary uncertainty quantification; and
6. *Realistic*: The algorithm should generate geologically plausible boundary models.

The explicit method is first described. The implicit method is then described; two currently available methods as well as the new *BOUNDSIM* method are presented. Table 1 shows a report card for evaluating these different boundary modeling methods.

Boundary Modeling Approach		Simplistic	Fast	Objective	Flexible	Access to Uncertainty	Geological
<i>Explicit</i>							
<i>Implicit</i>	<i>Leapfrog</i>						
	<i>Potential-Field</i>						
	<i>BOUNDSIM</i>						

Table 1: Report card for evaluating various boundary modeling algorithms in this work.

Explicit Boundary Modeling

The traditional approach to modeling ore-waste or hydrocarbon bearing boundaries is through a 3D triangulation of polygons or strings representing the solid body. The polygonal/string outlines or poly-lines are drawn by a geologist or engineer on a series of offset cross sections using expert judgment. The cross sections are then joined by tie-lines in order to guide the connectivity between poly-line sections during the 3D triangulation of the solid boundary. This procedure is referred to as an explicit model of the solid since the bounding surface is defined unequivocally by the 3D coordinates positioning the patchwork of triangles. Figure 3 illustrates the explicit boundary modeling procedure for a typical vein-type mineral deposit.

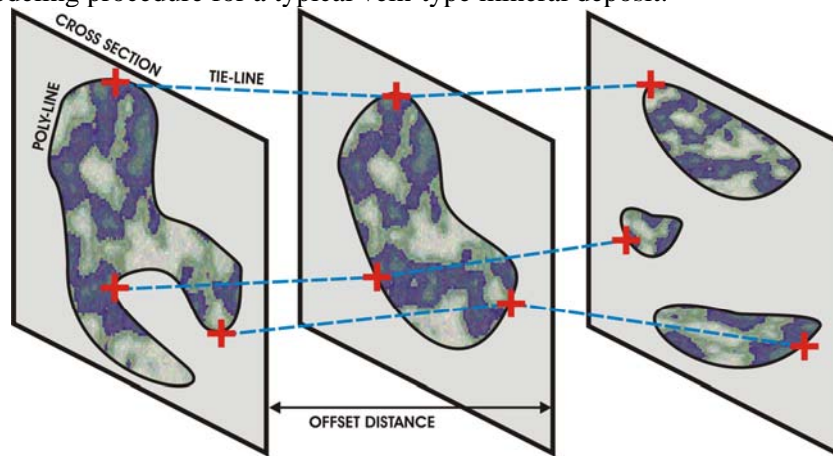


Figure 3: An illustration of the explicit boundary modeling method using poly-lines and tie-lines.

Although the explicit boundary modeling procedure is straightforward, there are a number of important limitations. These include significant time consumption, subjectivity and non-repeatability, inflexibility, and inability to access boundary uncertainty. Table 2 summarizes the report card for the explicit approach. Some comments then follow.

Boundary Modeling Approach		Simplistic	Fast	Objective	Flexible	Access to Uncertainty	Geological
<i>Explicit</i>		yes	no	no	no	no	yes
<i>Implicit</i>	<i>Leapfrog</i>						
	<i>Potential-Field</i>						
	<i>BOUNDSIM</i>						

Table 2: Report card for evaluating the explicit boundary modeling procedure.

Simplistic

Although the procedure may be tedious, the explicit method of digitizing polygons on several cross sections is definitely simple. Indeed, this is the main reason for its popular implementation in practice.

Time Consuming

Drawing the 2D poly-lines and tie-lines demands an overwhelming amount of time in many practical natural resource accumulations. For especially complex mineralization or layering with several intricate compartments of ore or hydrocarbon, it is not uncommon for a professional to spend up to three months developing a solid boundary model. There is certainly some shared aspiration to expedite this step in the overall workflow of a natural resource study.

Subjectivity and Non-Repeatability

The volume of mineralization is essentially composed of a prolonged series of small subjective or deterministic decisions as each corner of the poly-line from each cross section is chosen by a professional geologist or engineer. Inevitably, a signature of the interpreter is imparted to the boundary. For example, geologists, geophysicist, and engineers may all consistently generate significantly different boundary models given the same conditioning information. There is a need to generate objective boundary surfaces.

Inflexibility

It is very difficult to update an explicit boundary model upon the advent of new drillhole or well data. Typically, modifications are undertaken on campaigns [1]. There is a desire to immediately update boundary models as any new information becomes available.

Inaccessible Uncertainty

Since it is rather onerous to construct multiple explicit global accumulation boundary models, it is then difficult to assess the global uncertainty in these geometric limits between sample data. These uncertainties can be a major source of uncertainty in many situations. For example, with a vein-type gold deposit, the volume of mineralization is a vital economic indicator for project management. Ignoring the volumetric uncertainty by considering just one explicit boundary modeling may devastate the venture. There is a need to account for boundary uncertainty.

Geologically Realistic

Although explicit procedures are time consuming, subjective, non-repeatable, inflexible, and unable to fairly access global uncertainty, the resulting boundaries will be geologically realistic

especially when interpreted by the same individual generating the boundary. There is direct control of this goal in the digitization procedure.

Other than tediously redrawing all of the poly-lines and tie-lines and re-triangulating, there is no straightforward way to incorporate multiple possible boundary realizations representing uncertainty – this is indeed the single most important limitation of the explicit procedure.

Implicit Boundary Modeling

A new implicit surface modeling framework is developed. Sample drillhole or well data are used to interpolate what is referred to as a volume function. The boundary or zero-surface from the volume function is extracted at any desired resolution. Figure 4 shows a simple 2D example. The volume function interpolated from the sample data (circles) is shown at the top left. The color scale is symmetric ranging from highly negative (blue) to highly positive (red) values and is centered at zero (green). Three alternative boundary surfaces are extracted from this volume function at increasingly higher resolutions.

The advantages of the implicit boundary modeling approach can easily be seen through the small example in Figure 4. Alternative boundary geometries can be generated by interpolating the volume function at different resolutions, with different anisotropy, and with different expected values. Figure 4 illustrates the zero-surface boundary extracted from low, medium and high resolutions. As the resolution of the volume function increases, the boundary more closely honors sample and is smoother and perhaps more realistic. Anisotropic boundaries can be generated with anisotropic distance weighting for constructing the volume function. Inflated or contracted boundaries can be extracted from volume functions interpolated with higher or lower expected values. This last advantage is the essence for constructing probabilistic boundaries.

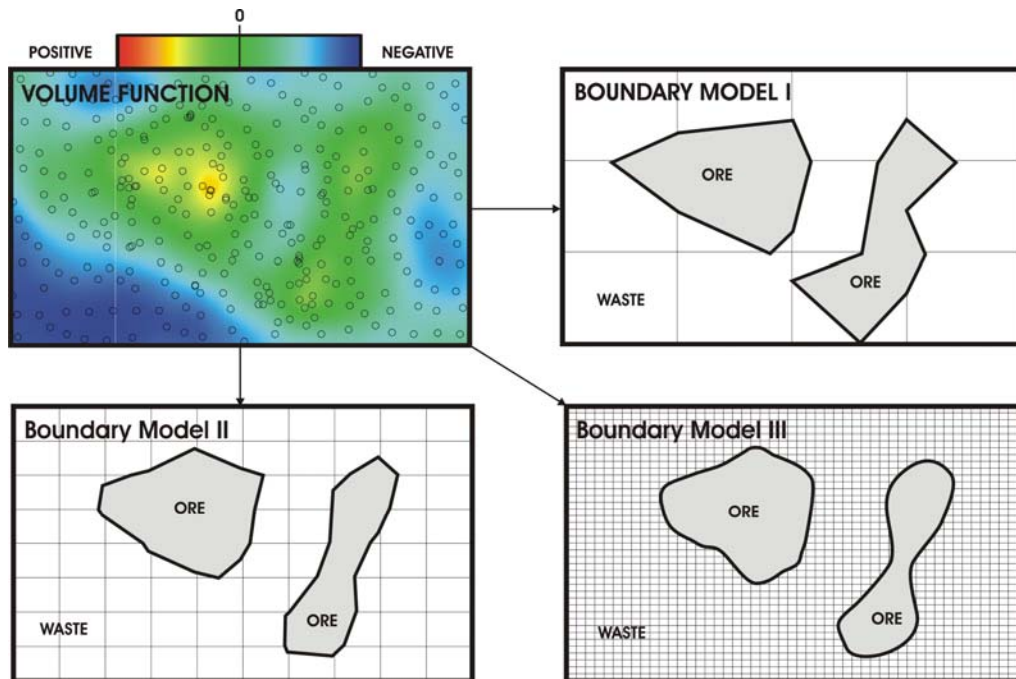


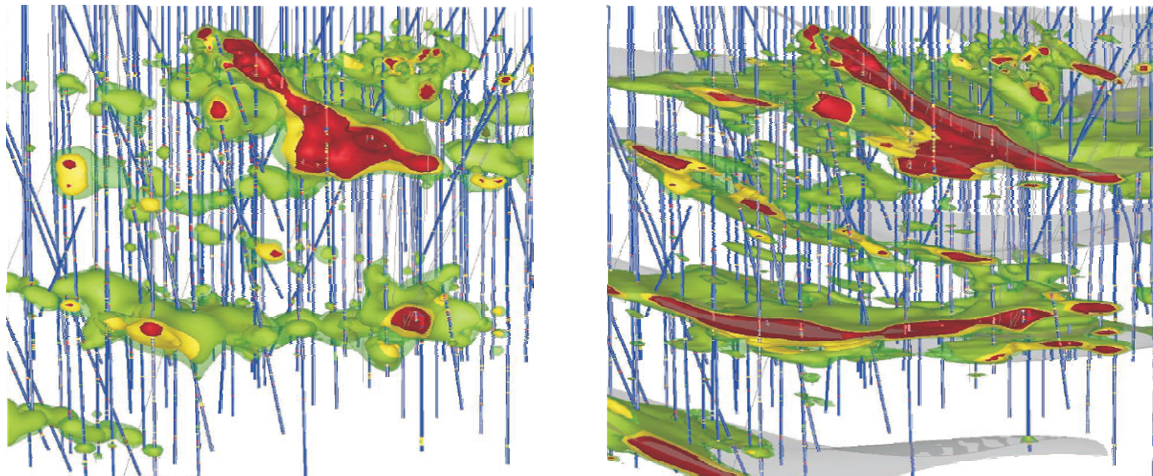
Figure 4: An illustration of the implicit boundary modeling method using a volume function and different extraction resolutions.

The implicit boundary modeling approach is fairly new in natural resource evaluation. However, there are a few well established implementations currently available. In this paper, we will review the *Leapfrog* [11, 12, 13] and *Potential-Field* [16] methodologies. Of course then the proposed *BOUNDSIM* methodology is presented in all necessary detail. These are then evaluated according to the criteria in Table 1.

Leapfrog Methodology

Leapfrog provides one of the first implicit boundary modeling implementations within a commercial software package. Overall, there are five major steps to the Leapfrog methodology: (1) data validation and compositing, (2) interpolation and meshing, (3) incorporating geological morphology, (4) interpolating the geological morphology, and (5) morphologically constrained interpolation. The method generates realistic boundary models consistent with the sample data and any possible morphological interpretation much quicker and more objectively than any explicit model. Figure 5 shows some grade boundaries generated by Leapfrog software for the Wallaby gold deposit, Australia. The grade boundaries on the left are interpolated without any geological interpretation whereas the boundaries on the right include the morphological shape constraints represented by the lightly shaded gray curvilinear planes.

The essential ingredient for implementing Leapfrog technology is the use of radial basis function (RBF) interpolation of the volume function [12, 14]. RBF interpolation is similar to the dual formulation of kriging where the estimates are weighted linear combinations of covariance functions [15]. In contrast to dual kriging, however, RBF interpolation does not derive the covariance functions from the data – they correspond to a simple isotropic linear covariance function. Therefore, there is no possibility of incorporating anisotropy into the boundaries through the RBF interpolation. Instead, it is injected manually in the form of deterministic morphological constraints.



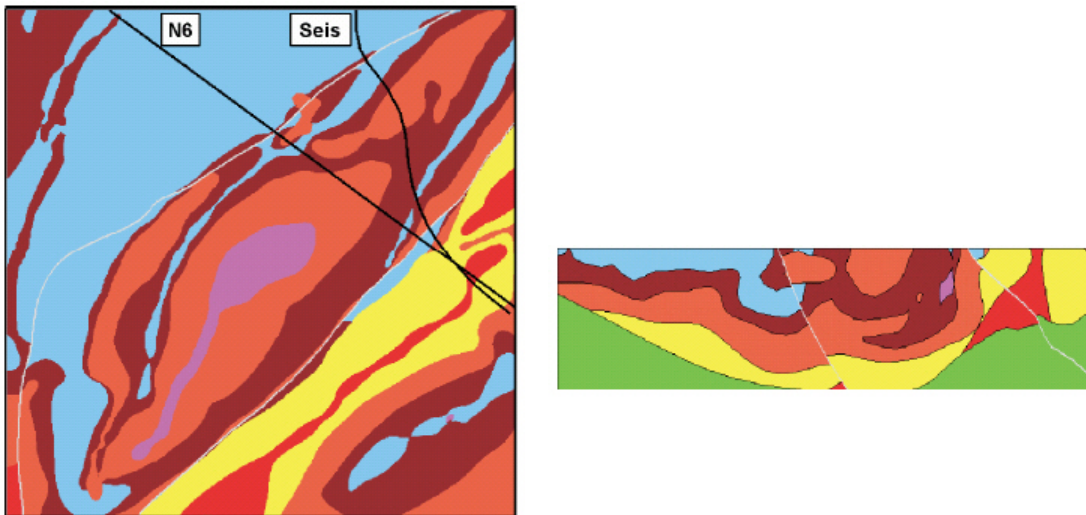
(Source: E J Cowan et al [13])

Figure 5: An illustration of implicit boundary modeling without (left) and with (right) geomorphologic constraints as implemented by Leapfrog software.

Leapfrog technology successfully overcomes many of the explicit boundary modeling limitations. The boundaries are certainly built quickly relative to the explicit method, the modeling process is objective and repeatable, and new sample and geological information can be easily incorporated. However, there is still no provision for the generation of multiple objective probabilistic boundaries representing the inherent uncertainty in these surfaces. Different boundary surfaces can be constructed based on different deterministic geological trends and morphological analyses; however, these interpretations still suffer from subjectivity and are not an objective quantifiable measure of boundary uncertainty. The implicit boundary modeling methodology presented in the next section will indeed allow for the quantification of this uncertainty.

Potential-Field Methodology

The Potential-Field is an implicit 3D scalar field from which a geological interface is extracted as a particular iso-surface. Overall, there are five major steps to the Potential-Field methodology: (1) collect surface intersection and structural orientation data, (2) determine the form of the locally varying drift, (3) infer the potential-field covariance function, (4) interpolate the potential field with a universal cokriging approach, and (5) visualize the uncertainty in the boundary surface placement. Figure 6 shows a plan view and cross section (at N6) through a 3D geological boundary model generated by the Potential-Field approach for the Broken Hill district. There are a total of seven different geological units. The white line represents the location of a fault and the black curved line is the location of a seismic line.



(Source: J P Chiles et al [16])

Figure 6: An illustration of implicit boundary modeling results with the Potential-Field method.

A key feature of the Potential-Field method is the use of universal cokriging to optimally account for both intersection and structural dip data. This approach is motivated by the fact that there are no direct samples of the potential field to condition a direct kriging. The structural data is interpreted as the gradient of the potential field. The execution of cokriging with gradient data is described in [15]. The method is not limited to intersection and structural data alone. Faults, seismic, and other available mining data can be incorporated into the interpolation procedure using a similar approach.

The Potential-Field methodology is quite flexible allowing various sources of data to enter into the interpolation of the potential field from which bounding surfaces are extracted. The boundaries are still built quickly relative to the explicit method, the modeling process is objective and repeatable, and various sources of geological information can be incorporated. However, the procedure is not simple. The covariance of the potential field is particularly difficult to infer since there are no hard potential field samples available.

Table 3 shows the report card for the Leapfrog and Potential-Field implicit boundary modeling methodologies. The explanation of these evaluations follows.

Boundary Modeling Approach	Simplistic	Fast	Objective	Flexible	Access to Uncertainty	Geological
<i>Explicit</i>	yes	no	no	no	no	yes
<i>Implicit</i>	<i>Leapfrog</i>	yes	yes	yes	yes	no
	<i>Potential-Field</i>	no	yes	yes	yes	yes
	<i>BOUNDSIM</i>					

Table 3: Report card for evaluating the Leapfrog and Potential Field implicit boundary modeling methods.

Simplicity

The implicit boundary modeling procedure is more sophisticated and challenging to implement properly. Collecting the conditioning data and interpolating a volume function involve some strong decisions about the geology of the deposit. The Leapfrog method can be implemented easily with the software available; however, the Potential-Field method is particularly challenging to implement.

Speed

Coding and interpolating the sample data to obtain the volume function or potential field are the most time consuming steps involved in the implicit method. However, this time commitment is practically reasonable and quite small relative to the alternative explicit approach. This relative advantage is the case especially for complex geological settings.

Objectivity and Repeatability

The explicit and implicit method must both necessarily create boundaries tied to some conditioning data. However, away from sample locations, explicit surfaces are digitized subjectively and manually whereas implicit surfaces are more objectively interpolated according to the estimation technique utilized. Although there are some choices involved in choosing and setting parameters for an interpolation technique, the extracted boundary surface depends solely on the resulting volume function. Of course, this more objective process can easily be automated and repeated since the estimation algorithm essentially remains the same.

Flexibility

The implicit method is extremely flexible. Different boundary geometries and sizes are integrated via the interpolation algorithm and can be extracted at any desired resolution. Various different sources and qualities of geological data and interpretation can be integrated. Updating an implicit boundary model upon the advent of new drillhole or well data is straightforward. Attribute grade boundaries can also be constructed.

Access to Uncertainty

The most important advantage of the implicit method is access to boundary uncertainty – explicit approaches are not capable of this. Nonetheless, the Leapfrog methodology does not provide any avenue for probabilistic boundaries accounting for uncertainty. The Potential-Field is capable of this through the kriging variance.

Geologically Realistic

Similar to explicit procedures, implicit boundary modeling methods are capable of geologically realistic bounding surfaces. The control over geological interpretation within the explicit method, however, is much higher than for more objective implicit methods.

The implicit *BOUNDSIM* algorithm described in this work passes all categories on the report card in Table 1. Unlike the Potential-Field method, it is relatively straightforward to implement and unlike the Leapfrog method, the emphasis is on probabilistic boundaries. *BOUNDSIM* is now described in all necessary detail.

***BOUNDSIM* Methodology**

There are seven major steps to the methodology: (1) make a decision of stationarity, (2) collect all sample and geological information, (3) code all the relevant sample data for conditioning volume function control points, (4) quantify the uncertainty in the expected volume function value, (5) decide on the domain, (6) interpolate the volume function control points within the domain, and (7) extract the boundary surface. The advantage of the *BOUNDSIM* methodology lies in step (4) and (6) where the ability to capture boundary uncertainty is incorporated.

The *BOUNDSIM* methodology is demonstrated with a simple 3D example. The example deals with a synthetically created spherical ore body within a typical *XYZ* coordinate system in units of meters (m). The spherical radius of the ore body is 20m. The grid resolution is 1m in each dimension. Figure 7 shows lower and upper *XY*, *XZ*, and *YZ* sections through this ore body. Since the ore body is symmetric in all sets of two dimensions, the cross sections are all and should all be the same. The model in Figure 7 represents the true underlying geology typically inaccessible in practice. In reality, only a limited number of samples or drillholes are available. A total of 100 exactly vertical drillholes are taken here. The assay data consists of a single indicator variable (0 for ore; 1 for waste) at the 1m grid resolution. Therefore, compositing is not necessary. The location of these 100 drillholes on the *XY* cross sections is shown in Figure 7.

The goal of the methodological presentation and this example is to model the true spherical boundaries. Of course, since there are only limited drillholes, the resulting boundary models will not be exactly spherical. Nonetheless, the uncertainty manifested from data paucity should and will be quantified. The *BOUNDSIM* implicit boundary modeling approach presented here is capable of quantifying this inherent uncertainty. Each of the seven steps mentioned above are now described in all necessary detail and illustrated with the example.

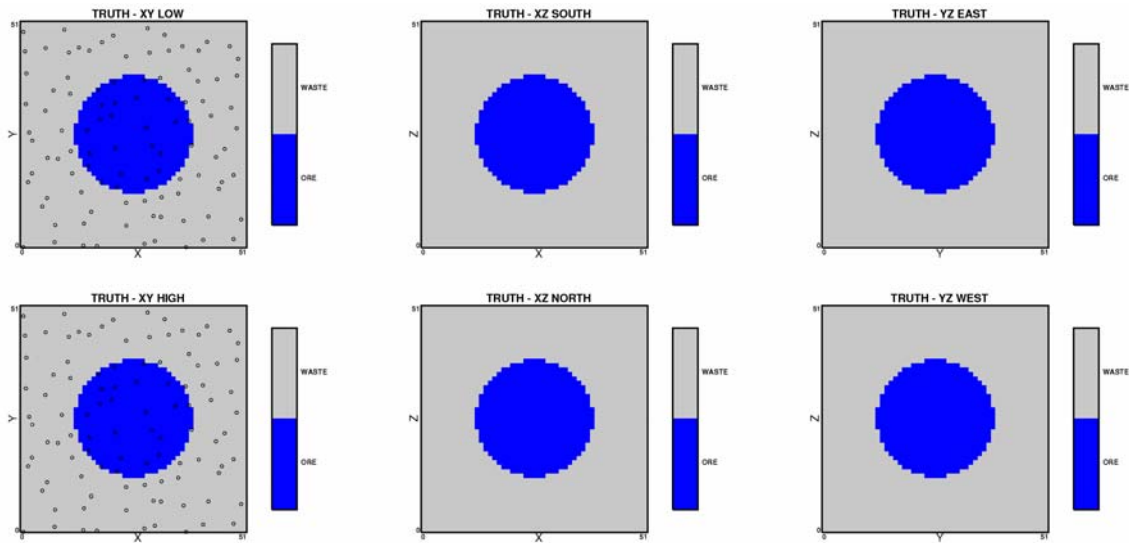


Figure 7: The true and practically inaccessible true spherical lithology model and 100 sample drillhole locations for the *boundsim* methodology example.

I. Decision of Stationarity

The first step of the procedure is to make a necessarily subjective decision of stationarity. These choices must always balance the degree of homogeneity and number of available data within potentially separate units of material. Consider the extremes. The most homogenous boundaries would surround any single sample datum; however, one sample is inadequate for accurately characterizing a stationary random function model applicable within such small boundaries. In contrast, by pooling all the data together, there may be an adequate database for reliable inference; but then there is also a significant risk of masking important heterogeneous features that could have otherwise been modeled by more than one stationary population. Each geological and engineering setting balances these two extremes uniquely. These decisions should be revised according to new geological information and/or sample data.

The decision of stationarity in this example is simple. Two homogeneous populations are decided on: ore and waste. The degree of homogeneity and pool of data within each assumed stationary population are both deemed sufficient in this scenario. In fact, all net (ore) vs. non-net (waste) boundary modeling problems like this example must adopt a similar decision of dual stationary populations. The modeling of boundaries certainly does not change this decision of stationarity – it merely defines the bounding surfaces that limit the spatial application of each corresponding stationary random function. The assay data within the ore and waste region would then be used to define the stationary random function and perform estimation and simulation within the limits defined by the boundary model.

A dual net to non-net or ore-waste type of stationarity decision fits in the second position before systems tract layer modeling and facies modeling in Figure 2. That is, the global accumulation limits (first stage) are set, the presence of systems tracts or other structural layering as well as facies is ignored, and just a net and non-net rocktype boundary is needed.

II. Geological Information

The data used to condition the boundary modeling procedure are an amalgamation of the subsets of data subsequently used to define the stationary random function model within the modeled boundary surfaces. It is essentially the spatial gradient between contrasting rocktypes that allows the implicit method to define and extract boundary surfaces. All 100 drillholes or 5100 rocktype samples are used to construct the ore-waste boundary model in the example. In practice, such drillhole data would be subjected to a lengthy process of compositing, cleaning, debiasing, visualization, and so on.

In practice, it is both *hard* and *soft* data that should be integrated into the boundary modeling procedure. Drillhole assays such as the rocktype variable in this example or grade attributes are generally referred to as *hard* data. Additional information contained in analog outcrops, stratigraphic interpretations, and seismic campaigns are generally referred to as *soft* data. Only hard rocktype variable data are considered in this example. The incorporation of soft data within the *BOUNDSIM* algorithm is a topic of future work.

III. Sample Data Codes

To construct an implicit model of a boundary surface, a volume function with an iso-surface that includes the contact points and points connecting them must be created [12]. This function is conditioned by control points coinciding with the drillhole or well string sample locations. However, the 0/1 indicator variable is incapable of defining a smoothly varying spatial volume function distribution from which a contour of zero iso-surface points can be defined and extracted. Separate regions must be specified where the volume function becomes increasingly positive and negative away from the desired boundary. And this requires the drillhole assays to be coded.

The volume function control codes are set to the distance between the sample location and the nearest different rocktype location. The sign of the distance depends on the rocktype being considered. If the location is within ore and the nearest rocktype is waste, the distance is negative; if the location is within waste and the nearest rocktype is ore, the distance is positive. Figure 8 shows the coded drillholes from Figure 1 and the distance sign rule used in the form of a decision matrix. The composites are taken at 1m.

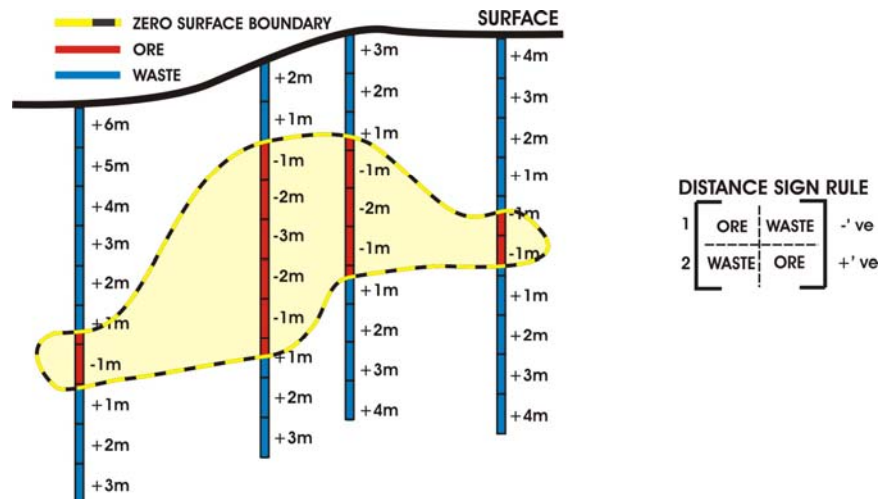


Figure 8: An illustration of the coding procedure to obtain volume function control points.

This coding scheme is now performed using all 100 drillholes for the ore-waste regions in the example. Figure 9 (left) shows the resulting distribution of volume function control points. Notice the distinct population of negative (inside [ore] bounds) and positive (outside [waste] bounds) control points. The average is +5.18 indicating that there is a more significant population of drillholes in waste. These distance codes will be interpolated on a Cartesian grid so that a locus of zero iso-surface points representing the ore-waste boundary can be defined and extracted according to the grid.

IV. Volume Function Uncertainty

The uncertainty in the mean volume function control needs to be established in order to generate probabilistic boundary models. This must be done before interpolating the volume function. An obvious, readily available, and robust technique for quantifying uncertainty in sample statistics like the mean is the bootstrap. Typically, the bootstrap resamples data with replacement for multiple realizations of the mean statistic as if the sample locations were spatially independent. However, regionalized variables such as rocktypes in this example are always spatially correlated. Therefore, the spatial bootstrap should be implemented in order to inject correlation into the otherwise random sampling of data [17].

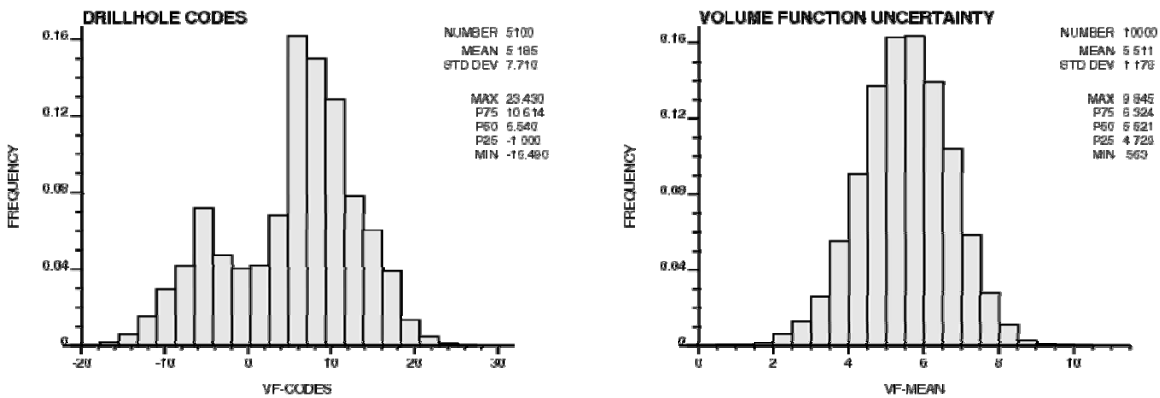


Figure 9: The distribution of conditioning volume function drillhole codes (left) and the distribution of uncertainty in the mean drillhole code value (right).

Figure 9 (right) shows the uncertainty in the volume function control mean using the spatial bootstrap. Based on the spatial correlation and drillhole paucity, the average volume function can range from 0.583 to 9.845. A smooth Gaussian variogram model with no nugget and 20m isotropic range identifies the model of spatial correlation.

The distribution in the right of Figure 9 is the critical link for generating probabilistic boundary models. Since the boundary is always extracted at the zero iso-surface contours, interpolating the volume function codes while honoring the different possible expected values in Figure 9 will effectively generate different probabilistic boundary surfaces. For example, a high risk boundary can be generated by choosing a very low quantile on this distribution which would effectively create a larger than expected boundary surface. A high volume function quantile can be chosen to generate lower risk or small boundaries.

V. Domain Size

In this example the domain size is fixed; however, in practice, this step in the *BOUNDSIM* algorithm is an important consideration. The global mineralization limits correspond to a cube 51m to each side.

Figure 10 shows the relationship between domain size and boundary geometry. The top row shows simple 2D cross sectional (*XZ*) reference boundary models built within 5 x 3km (left), 6 x 4km (middle), and 7.5 x 4.5km (right) domains. These rocktype models are then synthetically sampled on the same pseudo-regular 250m spacing from 0 to 5km in the *X* direction. These 20 drillholes are used to condition the construction of implicit boundary models for each case. The rocktype geometry, size, and relative position within each domain are the same – only the domain size changes. The *X* position of the 20 sample drillholes are also the same for each case. The second, third, and fourth rows of Figure 1 show the corresponding distributions of volume function codes, uncertainty in the mean volume function, and the interpolated volume function, respectively.

We might expect the size of ore pocket to decrease since the distribution of volume function codes is more negative. The negatives become more negative and the positives remain essentially the same for increasing domain sizes. Here however, the area of ore pocket does not fluctuate more than 5000m² (2 blocks) and the boundaries are virtually the same since the simple kriging interpolation algorithm consistently produces a mean volume function value of approximately -550 in each case. This is due to the requirement for a smooth search routine and spatial structure yielding little total weight to the mean. The boundary would indeed decrease in the presence of sparser sampling and subsequently higher weight to the mean. This insensitivity of simple kriging to the volume function mean is in fact another important challenge that needs to be addressed within the *BOUNDSIM* algorithm. One possible solution is post-processing the kriging map to honor the volume function mean explicitly.

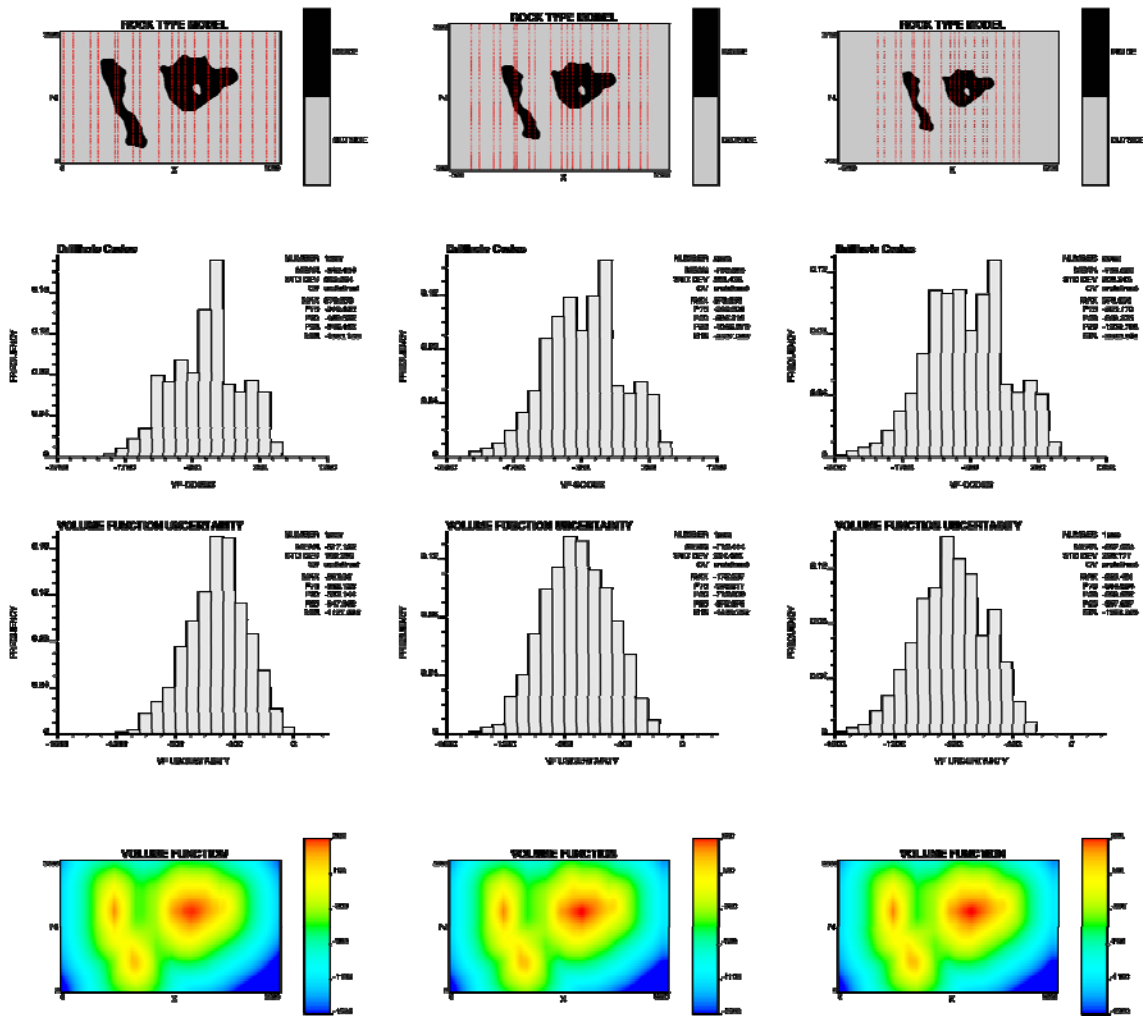


Figure 10: The relationship between domain size and boundary model geometry is investigated for a small 2D ore-waste cross sectional rocktype model. The same rocktype model and 20 X location drillholes are used in each case to construct the distribution of volume function codes, uncertainty in the mean volume function, and interpolated volume function (from top to bottom).

Notice also in Figure 10 the increase in volume function uncertainty as the domain size increases. Certainly the uncertainty is different for different domain sizes, that is, the width of distributions in the third row of Figure 10 is a function of the number of data or domain size. If data are sparse enough, the uncertainty translates to significantly different probabilistic boundaries. It is possible to use the different uncertainty to decide on the domain size ultimately used based on validation.

Probabilistic volume function models built using simple kriging are built with an attached degree of uncertainty. Simple kriging models this uncertainty by parameterizing the assumed normal distribution at every unsampled location with a kriging estimate and variance. One basic check is verifying that the resulting local probability intervals are consistent with the underlying model of uncertainty. For a specific probability interval (PI), p , we should expect to find that over multiple realizations, the proportion of times the true value falls within the PI is approximately equal to p for all p in $[0,1]$. For instance, a symmetric PI of 80% ($p = 0.80$) means that the lower and upper

probability values in the interval is 0.10 and 0.90, respectively. Ideally, the proportion of times the true value falls within the 80% PI should be close to 0.80. If this fraction is much greater than 0.80 then the probability interval is too wide and the local uncertainty may be too high. Conversely, if the fraction is much smaller than 0.80 then the probability interval is too narrow and the distribution has too low a variance. A cross plot of the true fraction vs. PI for a full range of PIs is known as an accuracy plot.

This procedure is performed for the volume function codes in Figure 10. The drillhole codes are transformed to normal score values so that a simple kriging will identify the local conditional normal distributions and the PI quantiles are known for checking accuracy. Figure 11 shows the accuracy plot for all three domain sizes (in the same order) previously shown in Figure 10. As expected from the increasing uncertainty in Figure 10, the local distributions of uncertainty grow wider and the accuracy plot rises with increasing domain size.

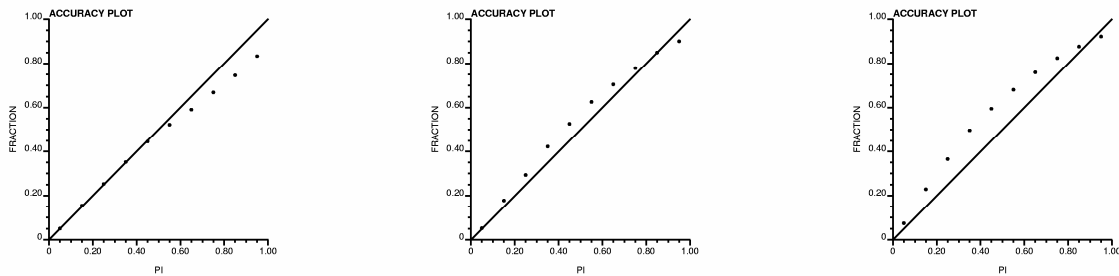


Figure 11: The accuracy plot for the interpolated volume function within each of the three domain sizes shown previously in Figure 10.

Figure 11 suggests the volume function uncertainty is more accurate and precise within the smaller 5 x 3km and 6 x 4km domains. However, the local distributions of volume function uncertainty are too wide for the largest 7.5 x 4.5km domain. This provides a framework for validating any boundary model and decision of stationarity that can be extracted from this volume function. At the same time, this validation provides a basis for choosing an appropriate domain size to model the subsequent boundaries within it.

VI. Volume Function Interpolation

The volume function control points must be interpolated from the drillhole locations throughout the entire global accumulation limits in order to define all possible extents of the boundary surface. This is done on a moderate resolution Cartesian grid network. The resulting volume function is in effect a gradient converging on a concentrated zero-value iso-surface boundary discretized by the resolution of the grid. The next step addresses the extraction of these zero-surface boundaries at any desired resolution. Of course, there remains to decide an appropriate interpolation method and parameters.

Simple kriging is chosen for interpolating the volume function due to its flexibility in the boundary modeling capacity. Simple kriging is a linear regression technique weighting surrounding conditioning data such that the expected variance of the estimation error is a minimum. The simple kriging weights and estimates account for the anisotropic spatial correlation of volume function codes and boundary models. Simple kriging also has the ability to honor different expected volume function values which allows the boundary surfaces to inflate or contract.

Applying the simple kriging interpolation of volume functions for boundary modeling is remarkably convenient. By specifying an anisotropic variogram model, one can change the geometry of the ensuing boundary surface. For example, an ellipsoidal boundary can be generated by specifying an anisotropic variogram while a more spherical boundary would be associated with an isotropic variogram. By specifying diverse expected volume function values, one can also generate different boundary surface sizes. For example, by inputting a lower (more negative) average volume function, the boundary surface and corresponding enclosed volume increases. This would correspond to an optimistic and high risk boundary, that is, a boundary where there is a high probability that the true bounding surface is smaller. Similarly, higher average volume functions are input to achieve more conservative and less risky boundaries. This remarkable flexibility is not available with the RBF approach.

Three sets of simple kriging runs are performed in this example. The same Gaussian variogram model with zero nugget and 20m isotropic range is used for all three volume functions since it is known the boundary is isotropic or spherical. This knowledge is analogous to *soft* geological information in practice. However, different average volume functions corresponding to the 10th, 50th, and 90th percentiles or p10, p50, p90 quantiles are honored by the kriging interpolation. These expected values are 3.99, 5.52, and 7.01, respectively.

Figures 12 to 14 show, for the same cross section orientations in Figure 7, the interpolated p10, p50, and p90 volume functions, respectively. In each figure, the volume function color scale ranges from -5.0 (blue) to +10.0 (red). The most important observation is perhaps the shrinking zero-valued boundary surface contour with decreasing risk going from Figure 12 to 14. Also notice that although an isotropic variogram model is used, the limited sample data do not generate perfectly spherical boundaries.

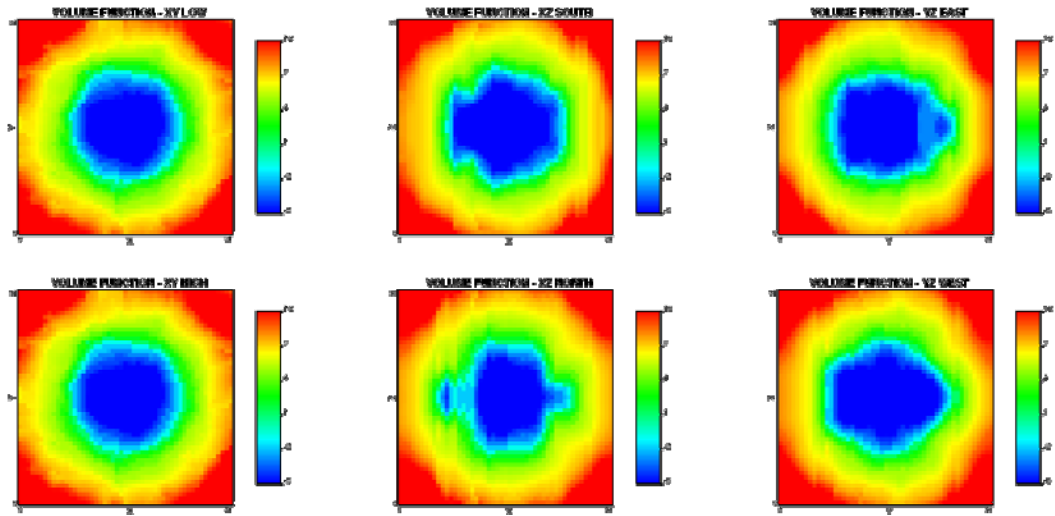


Figure 12: Interpolated volume function codes for the p10 boundary surface – aggressive risk.

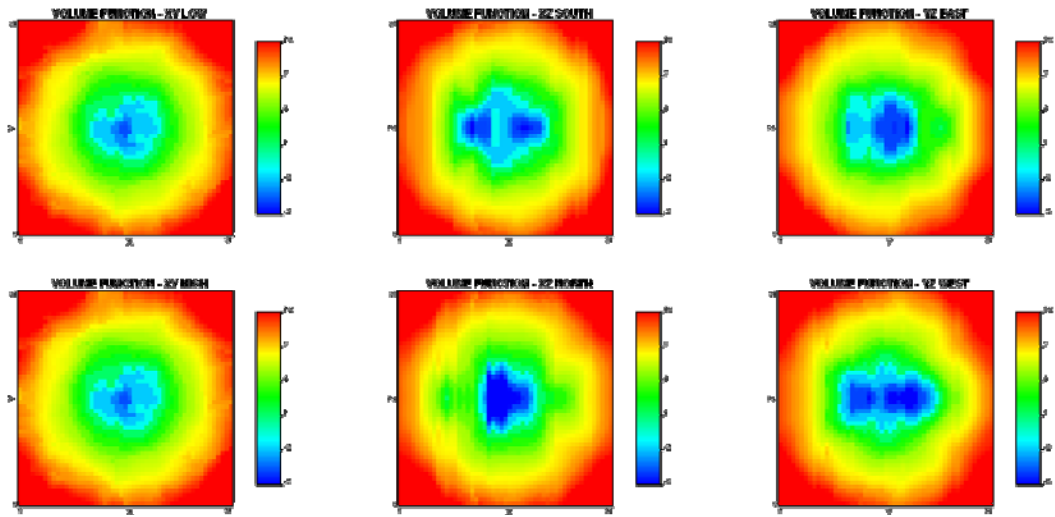


Figure 13: Interpolated volume function codes for the p50 boundary surface – moderate risk.

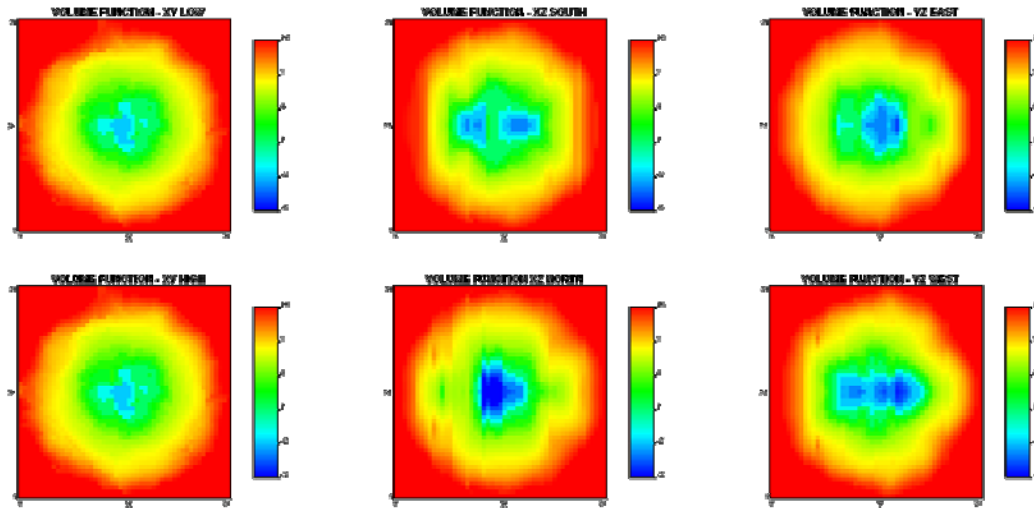


Figure 14: Interpolated volume function codes for the p90 boundary surface – conservative risk.

VII. Boundary Surface Extraction

The last step involves actually extracting the zero-value boundary surface contours from the volume function. Perhaps the simplest approach is importing the volume function from the previous step into a commercial software package and implementing a closed surface triangulation about the zero values. Although this is simple and direct, there is a necessary pre-processing step. Recall Figure 4 where different boundary surfaces are shown for different volume function resolutions. Higher resolutions are desirable for improved sample data reproduction and more realistic smooth boundaries. The problem is that the time and computer resources required to perform such a high resolution and necessarily smooth kriging run using a typical project database is often too demanding. The recommended approach for this *BOUNDSSIM* algorithm is to generate the volume function first at a moderate resolution then downscale the volume function to any desired resolution. The downscaled volume function can then be imported for triangulation.

For computer storage and speed considerations, the volume function is downscaled only at potential boundary margins. Figure 15 illustrates this downscaling procedure. A 27 cell (3 x 3 x 3) template is superimposed on each of the interpolated volume function grid cell values. Two such templates are shown in Figure 12 – the 3 layers of 9 cells are separated vertically here just for visualization purposes. The volume function sign in each template cell is indicated according to the position of the boundary surface element. A typical drillhole is also sketched in. Only connected cells hosting opposing volume function signs within these 27 cell templates are refined. All 26 possible connections to the center (6 face, 12 edge, and 8 diagonal) are considered. The refinement process is an inverse distance squared weighting of the 27 template volume function grid cell values as well as any drillhole data within the template boundaries.

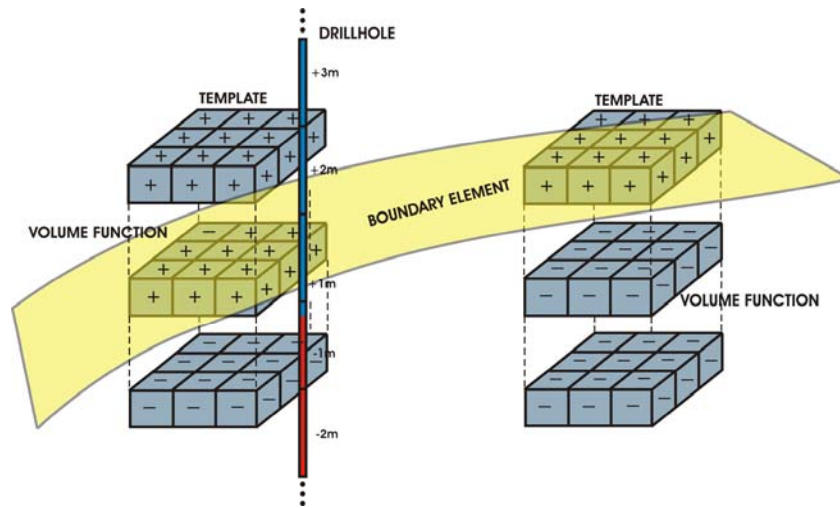


Figure 15: An illustration of the downscaling approach for the interpolated volume function.

The local boundary refinement procedure is applied to each of the p10, p50, and p90 boundary models. Figures 16 to 18 show the refined volume function within a more narrow volume function range of -2 (blue) to +2 (red). For enhanced visualization, these refined volume function blocks can be loaded into a commercial software package and triangulated. The high resolution zero iso-surface ensures data reproduction and realism.

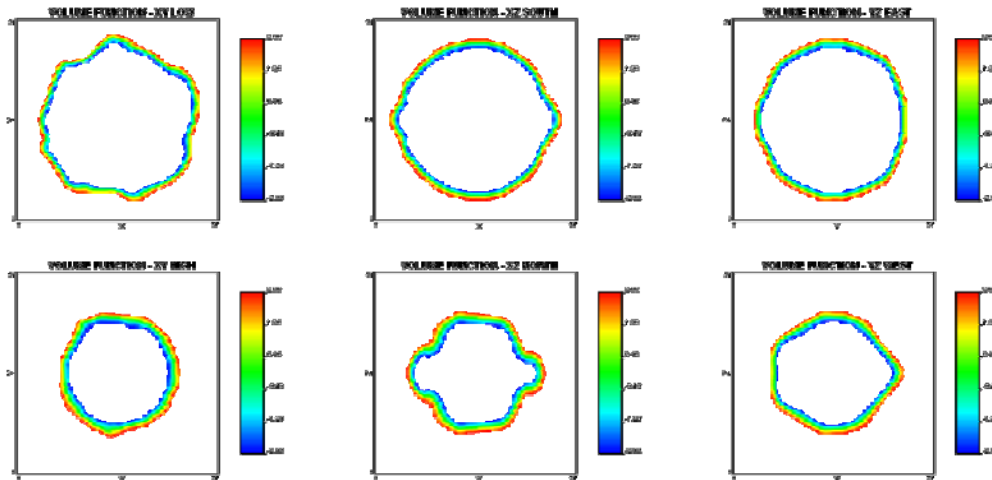


Figure 16: Refined volume function codes for the p10 boundary surface – aggressive risk.

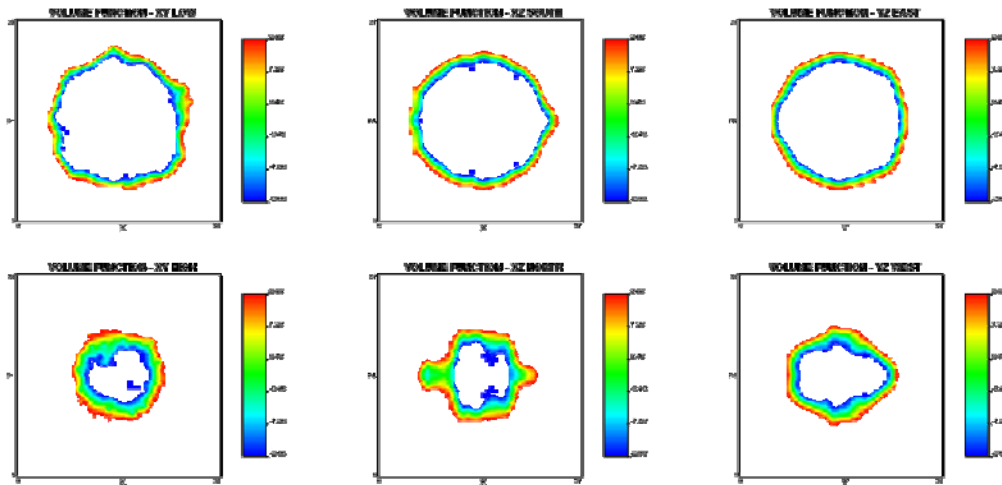


Figure 17: Refined volume function codes for the p50 boundary surface – moderate risk.

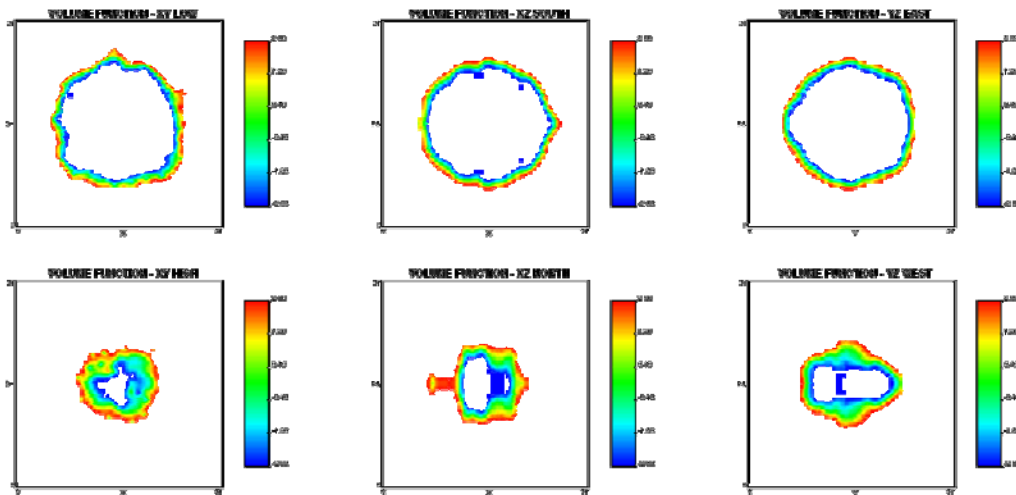


Figure 18: Refined volume function codes for the p90 boundary surface – conservative risk.

Future Work

There are a number of possible avenues for future research and development. These are discussed in this section.

So far *BOUNDSIM* is applied to net and non-net boundaries; however, there are many situations where more than two stationary populations are deemed homogeneous enough to model with separate random function models. The current binary approach could be nested according to some geological rules in order to model more than one boundary type.

The obvious next step for maturing the *BOUNDSIM* algorithm is applying the procedure to real boundary modeling problems. Vein type mineral deposits are of particular interest since the ore-waste boundaries in these settings are primary economic feasibility and production planning parameters. The uncertainty in such boundaries must be quantified. A small grade study could be

performed to assess the relative importance of boundary uncertainty versus different sources of uncertainty.

The implicit *BOUNDSIM* algorithm could also be applied in petroleum settings for systems tract or structural layer boundary modeling. A major difference between petroleum and mining problems is the relatively small number of available data. This makes parameters for kriging much more significant and motivates the integration of soft geological data and geomorphology trends. The *BOUNDSIM* procedure can even be applied for facies modeling.

The *BOUNDSIM* algorithm does not have to be applied to categorical variables. The same approach for coding drillhole data, interpolating a volume function, and extracting the zero boundary surfaces from this function is also applicable to continuous attribute grade models. Indeed, the construction of *grade shells* is a powerful visualization and production planning technique.

This paper presents a probabilistic framework for quantifying boundary uncertainty very simply controlled by specifying different expected volume function values from a possible distribution of uncertainty. However, an even more objective simulation framework can be developed to better capture the physical variation of the boundary between sample data. Sequential and truncated simulation techniques would be applicable in this capacity.

Other than specifying anisotropic boundaries through the variogram model, more advanced shape parameterization tools and controls are immediately available through the interpolation of the volume function with kriging. For example, universal kriging (UK) can be used to model boundaries according to a best fit deterministic function of the coordinates. This would be similar to the incorporation of deterministic geomorphology trends like the ones in Figure 5. Other possible techniques include non-stationary simple kriging and kriging with an external drift.

When there is uncertainty in the global accumulation boundaries, these can also be modeled with the *BOUNDSIM* approach. However, additional synthetic positive volume function drillhole codes would be needed in order to generate the gradients from negative and positive towards the zero value boundary contours.

Conclusion

A new solid modeling framework has been established and described in necessary detail. This implicit boundary modeling methodology *BOUNDSIM* is fast, objective and repeatable, flexible, and capable of accessing boundary uncertainty in a straightforward probabilistic manner. The basic algorithm is now well established. A number of promising research and development avenues have been identified. These will be developed as part of McLennan's thesis on stationarity.

References

- [1] Gemcom Software International Inc., Suite 1100 – 1066 West Hastings Street, Vancouver, British Columbia, V6E 3X1 Canada. *GEMS Suite of Software*. www.gemcomsoftware.com.
- [2] Maptek Inc., Suite 900, 165 South Union Blvd., Denver, Colorado, 80228 USA. *Vulcan Software*. www.vulcan3d.com.
- [3] Deutsch, C. *Geostatistical Reservoir Modeling*. Oxford University Press, 2002.

- [4] Chiles, J. and Delfiner, P. *Geostatistics: Modeling Spatial Uncertainty*. John Wiley and Sons, 1999.
- [5] Goovaerts, P. *Geostatistics for Natural Resources Evaluation*. Oxford University Press, 1997.
- [6] Deutsch, C.V. and Tran, T.T. *FLUVSIM: A Program for Object-Based Stochastic Modeling of Fluvial Depositional Systems*, Computers and Geosciences, 2002, vol. 28, pp. 525-535.
- [7] Pyrcz, M. and Deutsch, C.V. *ALLUVSIM: A Program for Streamline-Based Stochastic Modeling of Fluvial Depositional Systems*, Centre for Computational Geostatistics, Report 6, Edmonton, Alberta, September, 2004.
- [8] Xie, Y.L., Deutsch, C.V., and Cullick, S. *Surface-Geometry Simulation to Integrate Stratigraphic Surfaces in Subsurface Models*. Centre for Computational Geostatistics, Report 2, Edmonton, Alberta, September, 2000.
- [9] Pyrcz, M. and Deutsch, C.V. *Stochastic Surface Modeling in Mud-Rich Fine-Grained Turbidite Lobes*. Centre for Computational Geostatistics, Report 4, Edmonton, Alberta, September, 2002.
- [10] Pyrcz, M. and Deutsch, C.V. *SURFSIM: A Program for Stochastic-Based Simulation for Strataform Sediments*. Centre for Computational Geostatistics, Report 6, Edmonton, Alberta, September, 2004.
- [11] Cowan, E., Beatson, R., Ross, H., Fright, W., McLennan, T., Evans, T., Carr, J., Lane, R., Bright, D., Gillman, A., Oshust, P., and Titley, M. *Practical Implicit Geological Modeling*. The Australian Institute of Mining and Metallurgy Publication Series, no. 8, 2003.
- [12] Cowan, E., Beatson, R., Fright, W., McLennan, T., Evans, and Mitchell, T. *Rapid Geological Modeling*. Presented at Applied Structural Geology for Mineral Exploration and Mining International Symposium, Kalgoorlie, Australia, 2002.
- [13] Zaparo Ltd., 1060 Hay Street, Level 3, IBM Building, West Perth, Australia, WA 6005. *Leapfrog Software*. www.leapfrog3d.com.
- [14] Hardy, R. *Multiquadratic Equations of Topography and other Irregular Surfaces*. Journal of Geophysical Research, 1971, no. 176, 2002, pp. 1905-1915.
- [15] Chiles, J. and Delfiner, P. *Geostatistics: Modeling Spatial Uncertainty*. John Wiley & Sons, New York, 1999.
- [16] Chiles, J.P., Aug, C., Guillen, A., and Lees, T. *Modeling the Geometry of Geological Units and its Uncertainty in 3D from Structural Data: The Potential-Field Method*. Orebody Modeling and Strategic Mine Planning, Perth, Western Australia, 2004.
- [17] Deutsch, C.V. *A Statistical Resampling Program for Correlated Data: Spatial Bootstrap*. Center for Computational Geostatistics (CCG), Report 6, 2005.